

The reading operation of quantum dot memory devices using photocurrent detection in strain relaxation InAs quantum dots

Jia-Feng Wang, Cheng-Lu Lin, Sheng-Shiang Pan, Chih-Pin Huang, Chao-Sheng Hsieh and Jenn-Fang Chen

Department of Electrophysics, National Chiao Tung University,
1001 Da Hsueh Road, Hsinchu, 30050, Taiwan R.O.C.
Phone: +886-3-571-2121 E-mail: tonop98g@nctu.edu.tw

Abstract

We demonstrate the memory devices using the combination of the two devices, the GaAs Schottky diode and the InAs quantum dots (QDs) embedded in GaAs matrix. The photocurrent generated from the Schottky diode can be suppressed by the charged InAs QDs device behind. And further, the photocurrent can be controlled by the feedback between the two devices. The equivalent RC circuit model is provided in this paper, and the effective capacitance of the InAs QDs is obtained as about $0.1\mu\text{F}$. Besides, it is also proved that the strain relaxation QDs with misfit defect is more suitable to be fabricated as the quantum dot memory devices than the perfect non-relaxed QDs.

1. Introduction

Self-assembled InAs quantum dots (QDs) have applied to the quantum dot memory devices. The writing and erasing operations of the memory devices are operated by the carriers charging and discharging the InAs QDs. In general, the charged/discharged QDs represent 1/0 state of the memory cell. Most groups used the hysteresis in capacitance-voltage (C-V) or current-voltage (I-V) to detect the 1/0 state of the QDs, and the opening of the hysteresis is usually related to the amount of carriers trapped in the QDs. In this paper, we provide another method to discriminate the 1/0 state of the QDs. The QDs are connected with the Schottky diode, and the voltage divisions across the two devices mutually compensate to each other. The storage state of the QDs can be probed by detecting the voltage division of the Schottky diode. This method is rare in the past investigations.

2. Sample Fabrication and Properties

Three samples are discussed in this paper: reference sample with GaAs Schottky diode, non-relaxed QDs (thickness of QDs: 2.66 ML), and relaxed QDs (thickness of QDs: 3.33 ML). The two types of QDs samples are deposited on the n^+ -GaAs (100) substrate by molecular beam epitaxy (MBE). A $0.2\mu\text{m}$ Si-doping GaAs buffer layer ($6\times 10^{16}\text{cm}^{-3}$) was first grown at 580°C on the substrate, followed by a layer of InAs QDs, 2.66 ML (non-relaxed QDs) and 3.33 ML (relaxed QDs), grown at 500°C . A $0.3\mu\text{m}$ Si-doping ($6\times 10^{16}\text{cm}^{-3}$) top GaAs layer is grown to complete the structure. For the two QDs samples, the Schottky contacts are formed by evaporating Al on top, and the ohmic contacts are placed at the bottom using an In electrode. And then, the n^+ -GaAs substrate without any QDs fabrication is directly made to the reference sample, a Schottky contact is formed by evaporating Al on top and a Ohmic contact on bottom similarly.

It has been reported in our previous studies that the self-assembled InAs QDs relax when the deposited thickness of the QDs exceeds the critical thickness.[1] In addition, the strain relaxation induces a misfit defect at the bottom of the InAs QDs. This defect has been confirmed by transmission electron microscopy (TEM) images [2,3]. The misfit defect

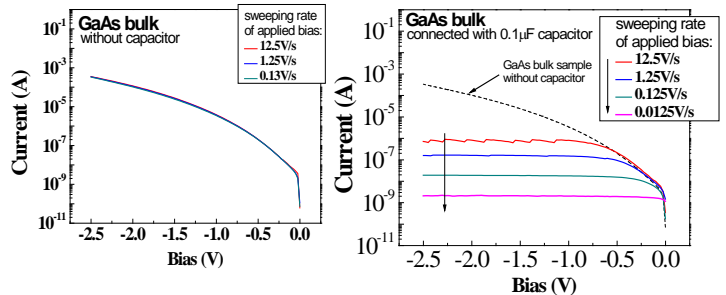


Fig. 1 The photocurrent of (a) GaAs bulk sample and (b) GaAs bulk sample connected with $0.1\mu\text{F}$ ceramic capacitor, under various sweeping rates of applied bias at room temperature.

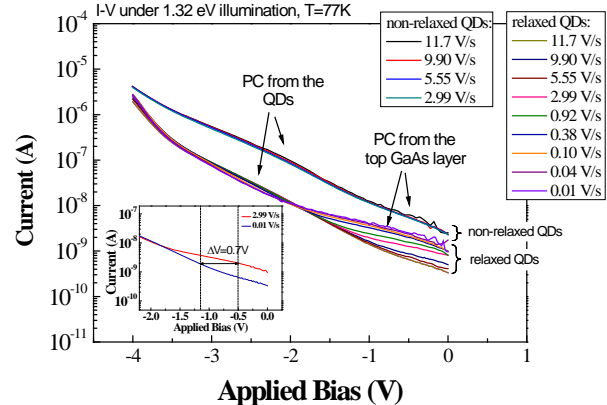


Fig. 2 The I-V for relaxed and non-relaxed QDs are shown. The insert is the amplified of relaxed QDs at small bias range.

also enhances the confinement of the QDs. The carriers are easily captured by the relaxed QDs than the non-relaxed QDs. [2] Further details about the relaxed and non-relaxed QDs can be found in Ref. [1-4].

3. Results and Discussion

The photocurrent of the GaAs bulk sample (reference sample) are shown in Fig. 1, where the illuminating energy is 1.32eV . We infer that the photocurrent is contributed from the deep level defect located at 1.3eV from the conduction band, and the defect is caused by the Ga vacancy in GaAs matrix.[5] The deep level defect plays a role as the generation-recombination center, if the defect is located in the depletion region. So the photocurrent is proportion to the depletion width, for the Schottky diode under reverse bias. In Fig.1-(a), the photocurrents are virtually fixed irrespective of the sweeping rate variation, and increase with the reverse bias. In Fig.1-(b), after connecting a $0.1\mu\text{F}$ ceramic capacitor in series, the photocurrents are shown in response to the various sweeping rates, and the photocurrent is suppressed with the slower sweeping rate. To consider the case of constant applied bias, the voltage division across the capacitor exponentially increases with a RC time constant, and the voltage division across the GaAs bulk sample decreases with time. The photocurrent from the GaAs bulk sample decreases due to the reduction in the potential. Therefore, the photocurrent can be

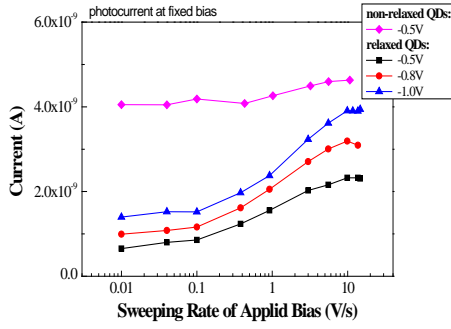


Fig. 3 The photocurrents are suppressed for the longer charging time.

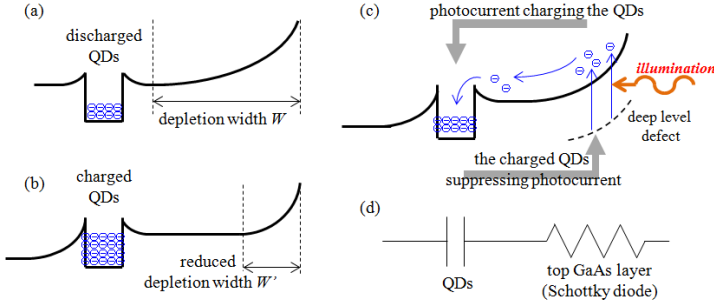


Fig. 4 (a)(b)The band bending of the top GaAs layer can be modulated by the charged QDs. (c) The feedback relationship between the two devices. (d) The equivalent RC circuit model of the QDs samples.

suppressed by the charged capacitor. Since the photocurrent is proportional to the depletion width, W , we can write

$$\frac{q}{2\epsilon} N_D W^2 = V_{bi} + V_R - \frac{1}{C} \int_0^{\Delta t} i(t) dt, \quad (1)$$

where N_D is the doping concentration, V_{bi} and V_R are the built-in potential and applied potential, and $i(t)$ is the charging current programmed into the capacitor. With the slower sweeping rate, the charging time Δt in eq.(1) is longer. The longer charging time means the capacitor has sufficient time to be charged, and produces a reduced W . Because the reduced W contributes a smaller photocurrent, the suppressed photocurrent is shown in Fig.1-(b) for slower sweeping rate.

The properties of the InAs QDs samples are similar to the RC circuit above. The structure of top GaAs layer in QDs samples is completely the same with the GaAs bulk sample, and the QDs with carrier storage are similar to the additional capacitor. The photocurrents under various sweeping rates for both QDs samples are shown in Fig. 2. The photocurrents at small bias ($0 \sim -1.5V$) are generated from the top GaAs layer, while the small bulges from $-2V$ to $-3V$ are attributed to the QDs. The photocurrents of relaxed QDs sample respond to the sweeping rate at the small bias range ($0 \sim -1.5V$). However, the currents for the non-relaxed sample are almost the same. That is because the two samples have different carrier confinement, the electron emission rate of relaxed QDs is 10^5 Hz and the emission rate of non-relaxed QDs surpasses 10^7 Hz.[2] The relaxed QDs play the role of a fully charged capacitor, but the electrons can easily tunnel out for the non-relaxed QDs. It is obvious that the capability of voltage modulation for the non-relaxed QDs is deprived.

In Fig. 3, the photocurrents at constant bias analysis for relaxed QDs under various sweeping rates are shown. The three ranges are discussed: (1) as the sweeping rate exceeds 10 mV/s, the photocurrent saturates at 3×10^{-9} A. The sweeping rate is so fast that the relaxed QDs have insufficient time to fill with carriers. The suppression effect of relaxed QDs is slight; (2) from 10 to 0.1 mV/s, the photocurrent begins to fall.

The few carriers are charged into the relaxed QDs as the increased charging time; and (3) From 0.1 to 0.01 mV/s, the relaxed QDs have sufficient time for the charging process to occur. The voltage division across the top GaAs layer is minimal and the suppression effect of relaxed QDs is evident.

The band diagrams described by eq.(1) are shown in Fig.4-(a) and (b). A large photocurrent can charge the QDs rapidly, but the charged QDs suppress the generation of photocurrent at the same time. So a feedback relationship exists between the two devices (as Fig.4-(c)). In fact, the final photocurrent in equilibrium is determined by three factors: the generation rate of photocurrent (R), the sweeping rate of applied bias (r_{SW}), and the electron emission rate of the QDs (C). The equilibrium photocurrent is obtained using the analysis of Kirchoff's law for the equivalent circuit (Fig.4-(d)), we derive:

$$i(V_R) = r_{SW} C \{1 - \exp[-V_R / r_{SW} RC]\} \quad (2)$$

The eq.(2) is determined by the three factor mentioned above (R , r_{SW} , and C), and this formula also is confirmed in Fig.1-(b) and the small bias region in Fig.2.

For the GaAs bulk sample (reference sample), the effective resistor is produced due to the current passing through the sample, such that the resistance is cursorily obtained to be about 10 M Ω from the I-V. The capacitance of the series connected ceramic capacitor is $0.1\mu F$. So the RC time constant is determined to be approximately 1 s. Fig. 3 indicates the charging time of the relaxed QDs is on the order of a few seconds (sweeping rate: $0.1 \sim 10$ V/s). So the effective capacitance of the relaxed QDs is obtained as $0.1\mu F$. The accurate capacitance can be determined further using the equation as below:

$$\Delta V = \frac{1}{C} [\int_0^{t_1} i_1(t) dt - \int_0^{t_2} i_2(t) dt] = \frac{1}{C} [Q_1 - Q_2] \quad (3)$$

Two I-V curves are chosen from Fig. 2 to analyze the charging process as the insert of Fig. 2. The ΔV rises due to the difference in the number of carriers between the two charging time. The capacitance of relaxed QDs is determined to be $0.089 \mu F$ using eq.(3).

4. Summary

We exhibit the photocurrent can be modulated by the relaxed QD. The formula of photocurrent and the effective capacitance of the relaxed QDs have been derived. Even though the charging time of the QDs is approximately 1 s in this paper, some investigations indicate that the charging time of the QDs can be reduced to below 6 ns.[6] This design allow the reading operation of quantum dot memory devices or detecting of other opto-electrical devices.

References

- [1] J. F. Chen, Y. C. Lin, C. H. Chiang, Ross C. C. Chen, Y. F. Chen, Y. H. Wu, and L. Chang, J. Appl. Phys. **111**,013709 (2012)
- [2] J. F. Chen, Y. Z. Wang, C. H. Chiang, R. S. Hsiao, W. H. Wu, L. Chang, J. S. Wang, T. W. Chi, and J.Y. Chi, Nanotechnology, **18** (2007) 355401
- [3] J. F. Chen, Ross C. C. Chen, C. H. Chiang, Y. F. Chen, Y. H. Wu, and L. Chang, Appl. Phys. Lett. **97**, 092110 (2010)
- [4] J. F. Chen, and J. S. Wang, J. Appl. Phys. **102**, 043705, (2007)
- [5] M. Kaminska, M. Skowronski, J. Lagowski, J. Lagowski, J. M. Parsey, and H. C. Gatos, Appl. Phys. Lett. **43**, 302 (1983)
- [6] M. Geller, A. Marent, T. Nowozin, D. Bimberg, N. Akcay, and N. Oncan, Appl. Phys. Lett. **92**, 092108 (2008)